Inorg. Chem. **2004**, *43*, 3521–3527

{*trans*-1,4-Bis[(4-pyridyl)ethenyl]benzene}(2,2′-bipyridine)ruthenium(II) Complexes and Their Supramolecular Assemblies with *β*-Cyclodextrin

Sergio H. Toma,[†] Miriam Uemi,[†] Sofia Nikolaou,[†] Daniela M. Tomazela,[‡] Marcos N. Eberlin,[‡] and Henrique E. Toma*,[†]

Instituto de Química, Universidade de São Paulo USP, Caixa Postal 26077, CEP 05513, São Paulo, SP, Brazil, and Instituto de Química, Universidade Estadual de Campinas, Campinas, SP, Brazil

Received October 24, 2003

Two novel ruthenium polypyridine complexes, $[Ru(bpy)_2Cl(BPEB)](PF_6)$ and $\{[Ru(bpy)_2Cl]_2(BPEB)\}(PF_6)_2$ (BPEB = *trans*-1,4-bis[2-(4-pyridyl)ethenyl]benzene), were synthesized and their characterization carried out by means of elemental analysis, UV–visible spectroscopy, positive ion electrospray (ESI-MS), and tandem mass (ESI-MS/MS) spectrometry, as well as by NMR spectroscopy and cyclic voltammetry. Cyclic and differential pulse voltammetry for the mononuclear complex showed three set of waves around 1.2 V ($Ru^{2+/3+}$), –1.0 V ($BPEB^{0/-}$), and –1.15 ($BPEB^{-/2-}$). This complex exhibited aggregation phenomena in aqueous solution, involving π–π stacking of the planar, hydrophobic BPEB ligands. According to NMR measurements and variable-temperature experiments, the addition of β-cyclodextrin (βCD) to $[Ru(bpy)_2Cl(BPEB)]^+$ leads to an inclusion complex, breaking down the aggregated array.

Introduction

This work deals with the coordination chemistry of ruthenium(II) polypyridine complexes (a, b) containing the linear, *trans*-1,4-bis[2-(4-pyridyl)ethenyl]benzene (BPEB) ligand.

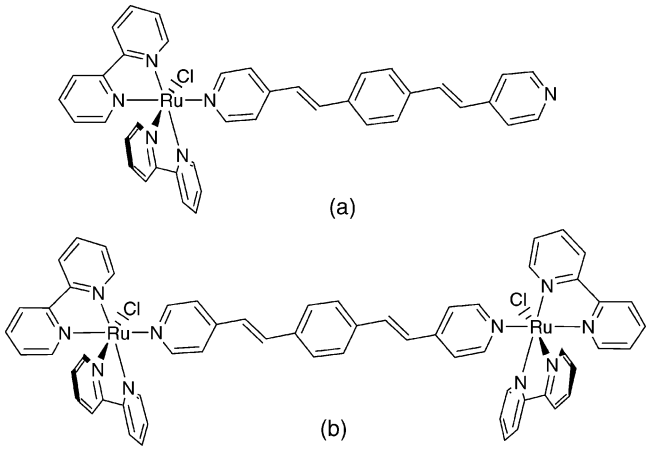

Ruthenium polypyridine complexes, such as $Ru(bpy)_3^{2+}$ (bpy = 2,2′-bipyridine) and its substituted derivatives, have been extensively studied in the past decades[1,2] because of their remarkable chemical and photochemical properties. On the other hand, BPEB is a typically conjugate bridging ligand, suitable to connect remote metal cores, allowing electron transport[3] as well as intramolecular photoinduced electron transfer or energy transfer processes.[2] Its structural features can also be exploited in the design of photoswitchable molecular devices.[4,5]

When combined to ruthenium polypyridine complexes, BPEB gives rise to a π-conjugated linear system, particularly interesting from the point of view of supramolecular chemistry. Inclusion compounds have been observed in this work, using cyclodextrins (CD), which are an important class of cyclic oligosaccharides composed of six (α-CD), seven (β-CD), or eight (γ-CD) D-(+)-glucopyranose units linked through α-1,4 glycosidic bonds, in a torus shape. In fact, these host molecules are able to accommodate a large variety of guests, including hydrocarbon surfactants,[6] aromatic

* Author to whom correspondence should be addressed. E-mail: henetoma@iq.usp.br.
[†] Universidade de São Paulo.
[‡] Universidade Estadual de Campinas.

(1) Juris, A.; Balzani, V.; Barigelletti, F.; Campagna, S.; Belser, P.; von Zelewsky, A. *Coord. Chem. Rev.* **1988**, *84*, 85.
(2) Balzani, V.; Scandola, F. *Supramolecular Photochemistry*; Ellis Horwood: Chichester, U.K., 1991.
(3) Ward, M. D. *Chem. Soc. Rev.* **1995**, 121.
(4) Yam, V. W.; Lau, V. C.; Wu, L. *J. Chem. Soc., Dalton Trans.* **1998**, 1461.
(5) Sun, S. S.; Lees, A. J. *Organometallics* **2001**, *21*, 31.
(6) Wilson, L. D.; Verral, R. E. *Can. J. Chem.* **1998**, *76*, 25.

10.1021/ic0352250 CCC: $27.50
Published on Web 05/04/2004

molecules,[7−9] water-insoluble drugs,[10−12] and inorganic compounds.[13−18] Such inclusion compounds result from the energetically unfavorable interaction between the included water molecules in the hydrophobic CD cavity on one hand and between water and guest on the other, in comparison with the hydrophobic and/or van der Waals interactions between the guest and the host cavity. Because of the specific interactions involved, this type of supramolecular system can be conveniently monitored by NMR spectroscopy.[19]

Another type of noncovalent intermolecular interaction particularly relevant in self-assembly is the $\pi-\pi$ stacking between aromatics units.[20,21] This type of interaction is expected to be particularly favored in BPEB containing systems, since this ligand is constituted by three aromatic rings held together by two ethylene bridges in a long, planar geometry. In the mononuclear $[Ru(bpy)_2Cl(BPEB)]^+$ complex, the ligand provides an extended aromatic residue which can not only be included into CD but also promotes molecular self-association by means of $\pi-\pi$ interactions between the stacked BPEB rings. The synthesis and characterization of the novel ruthenium polypyridyl complexes and the multiassembly behavior of the mononuclear complex $[Ru(bpy)_2Cl(BPEB)]^+$ in D_2O solution, as well the formation of its corresponding inclusion complex with β-cyclodextrin, are the subjects of this paper.

Experimental Section

Materials. All solvents and reactants were of analytical grade and employed without further purification. The starting $[Ru(bpy)_2Cl_2]\cdot 2H_2O$ compound was also obtained on the basis of a classical method reported in the literature.[22] β-Cyclodextrin was purchased from Aldrich and dried at 80 °C over vacuum at least 12 h before use.

Synthesis of *trans*-1,4-Bis[2-(4-pyridyl)ethenyl]benzene (BPEB). This ligand was prepared by the Heck method[23,24] and purified by recrystallization from a hot ethanol−water mixture. Anal. Found: C, 83.4; H, 5.8; N, 9.7. Calcd for $C_{20}H_{16}N_2$ (MW = 284.36): C, 84.5; H, 5.7; N, 9.6. Observed $[M + H]^+$: *m*/*z* 285.12.

Synthesis of $[Ru(bpy)_2Cl(BPEB)]PF_6$. The mononuclear ruthenium complex was obtained by the condensation of $[Ru(bpy)_2Cl(H_2O)]^+$ with BPEB in 6-fold excess, as follows: $[Ru(bpy)_2Cl_2]\cdot 2H_2O$ (226.5 mg; 0.44 mmol) was dissolved in 15 mL of 1:1 H_2O/MeOH argon-saturated solution and heated, while $AgNO_3$ (68.0 mg; 0.40 mmol) dissolved in 3 mL of deionized water was added. The mixture was heated at reflux for 15 min under an argon atmosphere. The AgCl precipitate formed was filtered off, and the dark brown solution was transferred to a two-necked round-bottom flask containing BPEB (742.6 mg; 2.61 mmol) in 200 mL of MeOH. After being refluxed for 1 h, the resulting solution was cooled at room temperature and added dropwise to an ammonium hexafluorophosphate solution (748.0 mg; 4.40 mmol). After the mixture was kept overnight in the refrigerator, the solid residue solid was collected on a filter, washed with few portions of cold water and diethyl ether, and dried in a vacuum. Further purification was performed by gradient elution in a chromatographic column, using neutral alumina (Brockmann activity I, 150 mesh) as the stationary phase and CH_3OH/CH_2Cl_2 mixtures as eluent. By an increase of the CH_3OH amount in the mixture, the BPEB ligand eluted first, followed by the unreacted ruthenium complex. When the CH_3OH/CH_2Cl_2 mixture reached 5% (v/v), elution of the complex was observed, yielding an orange-brown band. After removal of the solvent in a rotary evaporator, the solid residue was dried in a vacuum desiccator, until constant weight, in the presence of anhydrous calcium chloride (η = 68%). Anal. Found: C, 54.6; H, 4.3; N, 9.3. Calcd for $C_{40}H_{32}N_6PF_6ClRu$: C, 54.7; H, 3.8; N, 9.6. MS: calcd for $C_{40}H_{32}N_6ClRu$, *m*/*z* 733.14; obsd, *m*/*z* 733.29.

Synthesis of $[\{Ru(bpy)_2Cl\}_2(BPEB)](PF_6)_2$ (2). The binuclear complex was similarly prepared, using the method described as follows: $Ru(bpy)_2Cl_2\cdot 2H_2O$ (780.6 mg; 1.5 mmol) dissolved in 40 mL of 1:1 H_2O/MeOH was treated with $AgNO_3$ (237.8 mg; 1.4 mmol) for 15 min, under an argon atmosphere. The AgCl precipitate was filtered off, and the dark brown solution was added to 50 mL of a methanol solution containing BPEB (142.2 mg; 0.5 mmol). After being refluxed for 1.5 h, the solution was cooled to room temperature and then added dropwise to an ammonium hexafluorophosphate solution (1,63 g; 10 mmol). The precipitate was collected on a filter, washed with few portions of cold water and diethyl ether, and dried in a vacuum in the presence of silica gel. Further purification was carried by gradient elution in a chromatographic column, using neutral alumina (Brockmann activity I, 150 mesh) as stationary phase and mixtures of CH_3OH/CH_2Cl_2 as eluent (η = 42%). Anal. Found: C, 48.6; H, 3.6; N, 9.6. Calcd for $C_{60}H_{48}N_{10}P_2F_{12}Cl_2Ru_2$: C, 49.0; H, 3.3; N, 9.5. MS: calcd for $C_{60}H_{48}N_{10}Cl_2Ru_2$, *m*/*z* 591.08; obsd, *m*/*z* 591.24.

Instrumentation and Methods. Electrospray mass spectra were recorded on a high-resolution Q-Tof (Micromass, U.K.) mass spectrometer with a quadrupole (Qq) orthogonal time-of-flight configuration. The sample was introduced using a syringe pump (Harvard Apparatus, Pump 11) set to 10 μL/min through an uncoated fused-silica capillary. The sample was dissolved in pure methanol. The ESI spectrum was acquired using a capillary voltage of 3 kV and a cone voltage of 20 V.

Cyclic (CV) and differential pulse (DPV) voltammograms were carried out with a Princeton Applied Research model 283 potentiostat. A platinum disk electrode was employed for the measure-

(7) Dikavar, S.; Maheswaran, M. M. *J. Inclusion Phenom.* **1997**, *27*, 113.
(8) Salvatierra, D.; Jaime, C.; Virjili, A.; Sánchez-Ferrando, F. *J. Org. Chem.* **1996**, *61*, 9578.
(9) Mirzoian, A.; Kaifer, A. E. *Chem.—Eur. J.* **1997**, *3*, 1052.
(10) Loukas, Y. L. *J. Pharm. Pharmacol.* **1997**, *49*, 944..
(11) Oh, I.; Lee, M.; Lee, Y.; Shin, S.; Park, I. *Int. J. Pharm.* **1998**, *175*, 215.
(12) Djedaini, F.; Lin, S. Z.; Perly, B.; Wouessidjewe, D. *J. Pharm. Sci.* **1990**, *79*, 643.
(13) (a) Baer, A. J.; Macartney, D. H. *Inorg. Chem.* **2000**, *39*, 1410. (b) Wylie, R. S.; Macartney, D. H. *Inorg. Chem.* **1993**, *32*, 1830.
(14) Harada, A. *Acc. Chem. Res.* **2001**, *34*, 456.
(15) Nepogodiev, S. A.; Stoddart, J. F. *Chem. Rev.* **1998**, *98*, 1959.
(16) (a) Haider, J. M.; Chavarot, M.; Weidner, S.; Sadler, I.; Williams, R. M.; De Cola, L.; Pikramenou, Z. *Inorg. Chem.* **2001**, *40*, 3912. (b) Nelissen, H. F. M.; Kercher, M.; De Cola, L.; Feiters, M. C.; Nolte, R. J. M. *Chem.—Eur. J.* **2002,** *8*, 5407.
(17) Shukla, A.; Bajaj, H. C.; Das, A. *Angew. Chem., Int. Ed.* **2001**, *40*, 446.
(18) (a) Johnson, M. D.; Reinsborough, V. C.; Ward, S. *Inorg. Chem.* **1992**, *31*, 1085. (b) Ando, I.; Ujimoto, K.; Kurihara, H. *Bull. Chem. Soc. Jpn.* **2001**, *74*, 717.
(19) Scheider, H.-J.; Hacket, F.; Rüdiger, V.; Ikeda, H. *Chem. Rev.* **1998**, *98*, 1755.
(20) Bergaman, S. D.; Reshef, D.; Groysman, S.; Goldberg, I.; Kol, M. *Chem. Commun.* **2002**, 2374.
(21) (a) Bolger, J.; Gourdon, A.; Ishow, E.; Launay, J.-P. *Inorg. Chem.* **1996**, *35*, 2937. (b) Ishow, E.; Gourdon, A.; Launay, J.-P.; Chiorboli, C.; Scandola, F. *Inorg. Chem.* **1999**, *38*, 1504.
(22) Sullivan, B. P.; Salmon, D. J.; Meyer, T. J. *Inorg. Chem.* **1973**, *12*, 2371.
(23) Heck, R. F. *Org. React.* **1981**, *27*, 345.
(24) Amoroso, A. J.; Thompson, A. M. W. C.; Maher, J. P.; McCleverty, J. A.; Ward, M. D. *Inorg. Chem.* **1995**, *34*, 4828.

ments, using the conventional Luggin capillary arrangement in a DMF solution containing 0.100 mol dm^{-3} tetrabutylammonium hexafluorophosphate ((TBA)PF_6). The reference electrode was Ag/$AgNO_3$ (0.010 mol dm^{-3}) in acetonitrile containing 0.100 mol dm^{-3} (TBA)PF_6. A platinum wire was used as the auxiliary electrode. All the $E_{1/2}$ values presented here were converted to SHE by adding 0.503 V to the experimentally obtained values. Cyclic and differential pulse voltammetry scan rates were 100 and 9 mV/s, respectively. A three-electrode system with a gold minigrid transparent working electrode, mounted inside a conventional quartz cell with restricted internal optical path length (0.025 cm), was used for the spectroelectrochemical measurements. UV−visible spectra were recorded on a Hewlett-Packard model 8453 diode array spectrophotometer using 10^{-5} mol dm^{-3} solutions.

NMR experiments were recorded on a DRX 500 MHz Bruker spectrometer, except for the ^{1}H spectra used to construct the Job plots, which were carried out in a INOVA-1 300 MHz Varian spectrometer. The NMR chemical shifts are reported in parts per million (ppm) relative to residual protiated solvents ($\delta = 2.05$ ppm for acetone-d_6 and $\delta = 4.80$ ppm for D_2O) or relative to ^{13}C ($\delta =$ 206.17 and 29.84 ppm for acetone-d_6). [Ru(bpy)$_2$Cl(BPEB)]$^+$ concentrations ranging from 1 to 10 mmol dm^{-3} in D_2O were applied in studies focusing on the aggregation and inclusion phenomena.

The stoichiometry of β-CD inclusion compound was obtained by means of the continuous variation method (Job's method).[25,26] In this method the total concentration of the species ($[S]_0 + [L]_0 = M$) is kept constant, and the ratio ($r = [S]_0/\{[S]_0 + [L]_0\}$) between the S (Ruthenium complex) and L (β-CD) species varied from 0 to 1. The maximum complex concentration is reached for $r = (n + 1)^{-1}$ and does not depend on the concentration M or the binding constant (K_a).

In NMR studies, the continuous variation method makes use of the difference in the chemical shifts($\Delta\delta = \delta_0 - \delta$) of the ligand (or substrate) in a fast chemical exchange regime. In this sense, the chemical shift observed for a given nucleus can be expressed as function of the mole fraction of the species L and SL, e.g.

$$\delta_0 = f_L\delta_L + f_{SL}\delta_{SL}$$

where $f_L = [L]/[L]_0$ and $f_{SL} = [SL]/[L]_0$; δ_L and δ_{SL} are the chemical shifts of the β-CD (L) and the inclusion [Ru(bpy)$_2$Cl(BPEB.β-CD)]$^+$ complex (SL), respectively. Thus, the experimentally observed parameter (e.g. the chemical shift of the ligand) is sensitive to the complex formation. By the plotting of $\Delta\delta$ [L] versus the mole fraction of the ligand (r), the maximum is reached at the stoichiometry ($r = [n + 1]^{-1}$) of the inclusion complex.

The inclusion constant (K_a) for the [Ru(bpy)$_2$Cl(BPEB·β-CD)]$^+$ complex was determined from direct spectrophotometric measurements at $\lambda = 400$ nm, using a large excess of β-CD (e.g. 10-fold excess). The temperature and ionic strength were kept constant at 25.0 ± 0.1 °C and 0.1 M NaCl. In the determination of K_a we assumed the following equilibrium:

$$S + L \rightleftharpoons SL$$

Here the [Ru(bpy)$_2$Cl(BPEB)]$^+$ complex, β-CD, and [Ru(bpy)$_2$Cl(BPEB·β-CD)]$^+$ refer to the substrate (S), ligand (L), and the inclusion complex (SL), respectively. The absorbance of the substrate in the presence of CD is given by

$$A = \epsilon_S b[S] + \epsilon_L b[L] + \epsilon_{SL} b[SL] \quad (1)$$

Making use of mass balance for the ligand and substrate:

$$A = \epsilon_L b[L]_0 + \Delta\epsilon_{SL} b[SL] \quad (2)$$

Here $\Delta\epsilon_{SL} = \epsilon_{SL} - \epsilon_S - \epsilon_L$. Combining eq 2 with the K_a definition and after rearranging yield

$$\frac{\Delta A}{b} = \frac{\Delta\epsilon_{SL} K_a [S][L]_0}{1 + K_a[S]} \quad (3)$$

Equation 3 describes the absorption changes for a 1:1 complexation process. Several related methods can also be proposed. For instance, in the Scatchard[27] method, eq 3 becomes

$$\frac{\Delta A}{b[S]} = -\frac{\Delta A K_a}{b} + \Delta\epsilon_{SL} K_a [L]_0 \quad (4)$$

By the plotting of $\Delta A/b[S]$ against $-\Delta A/b$, the slope is given by K_a and $\Delta\epsilon_{SL}$ can be obtained by extrapolation to infinite dilution.

Results and Discussion

ESI-MS and MS/MS Structural Diagnostic Results. Electrospray ionization (ESI)[28] has revolutionized the way molecules are ionized and transferred to mass spectrometers, expanding the applicability of mass spectrometry for a variety of compounds with thermal instability, high polarity, and mass. Although ESI and tandem mass spectrometry have been mainly (and most successfully) applied to analyze biomolecules,[28] they are increasingly being used as powerful structural diagnostic techniques for inorganic and organometallic compounds.[29−30] The positive ESI mass spectra obtained from the mononuclear and binuclear complexes in methanol solution show [Ru(bpy)$_2$Cl(BPEB)]$^+$ and {[Ru(bpy)$_2$Cl]$_2$(BPEB)}$^{2+}$ as multiple-component, singly and doubly charged isotopomeric ions, centered at m/z 733.29 and 591.24, respectively. The ion abundance and m/z distribution matches perfectly the calculated isotopic pattern (not shown). The complex isotopic pattern observed results mainly from the presence of isotopic ruthenium atoms [Ru possesses seven isotopes: ^{104}Ru (18.7%), ^{102}Ru (31.6%),^{101}Ru (17.0%), ^{100}Ru (12.6%), ^{99}Ru (12.7%), ^{98}Ru (1.88%), ^{96}Ru (5.52%)].

For refined tandem mass spectrometry structural characterization, the gaseous ions of both complex centered at m/z 733.29 and 591.24, respectively, were mass-selected for collision-induced dissociation (CID). The product ion mass spectrum of the binuclear complex can be seen in Figure 1. It shows double- and single-charged ionic complexes formed by characteristic charge splitting ($M^{2+} \rightarrow F_1^+ + F_2^+$) and ligand loss dissociation, as depicted in Figure 2. Therefore, this characteristic dissociation pattern observed for the

(25) Job, P. *Ann. Chim.* **1928**, 9, 113−134.
(26) Fielding, L. *Tetrahedron* **2000**, 56, 6151−6170.
(27) Scatchard, G. *Ann. N.Y. Acad Sci.* **1949**, *51*, 660.
(28) Cole, R. B. *Electrospray Ionization Mass Spectrometry*; Wiley: New York, 1997.
(29) Colton, R.; D'Agostinho, A.; Traeger, J. C. *Mass Spectrom. Rev.* **1995**, *14*, 79.
(30) Nikolaou, S.; Uemi, M.; Toma, H. E. *Spectrosc. Lett.* **2001**, *34*, 267.

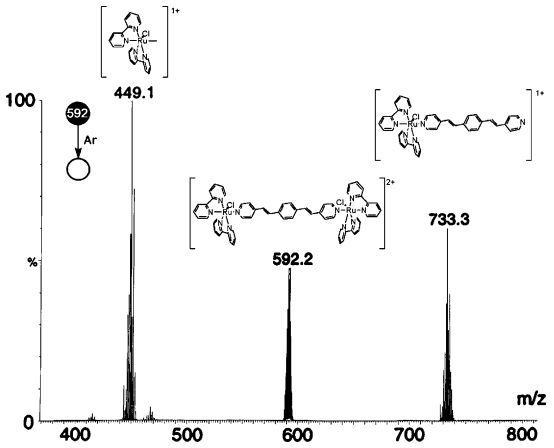

Figure 1. Tandem product ion mass spectrum for the mass-selected ionic $\{[Ru(bpy)_2Cl]_2(BPEB)\}^{2+}$ (**2**) centered at *m*/*z* 592. The ion shows a structural diagnostic dissociation behavior with characteristic charge splitting and ligand loss dissociation.

gaseous $\{[Ru(bpy)_2Cl]_2(BPEB)\}^{2+}$ species provides reliable pieces of evidence for its structural elucidation.

NMR Spectroscopy. The ^{1}H NMR spectra of the monomeric and dimeric ruthenium species exhibited up to 24 signals, as shown in Figure 2. In both complexes the bipyridyl protons displayed almost identical chemical shifts, ranging between 6 and 10.5 ppm. The major dissimilarity observed in these complexes is associated with the BPEB protons, responsible for 5 characteristic signals ascribed to α and β pyridyl, ω_1 and ω_2 ethenyl, and γ benzilic protons. All proton signals of the monomeric and binuclear complexes were assigned on the basis of ^{13}C NMR, ^{1}H$-^1$H COSY, and ^{1}H$-^{13}$C HMQC correlation spectra, as well as by comparison with related systems from the literature[30−32] (data available as Supporting Information).

In both complexes, large diamagnetic current effects were observed for the protons located just over the aromatic rings. In particular, the ring current effects from the bipyridyl ring fragment containing the protons labeled as **3**−**6** (Figure 2) are expected to exert direct influence on proton **10**. Likewise, proton **6** is located over the BPEB pyridyl group, undergoing upfield shift (shielding). Analogously, the **7**′, **8**′, **9**′, and **10**′ ring should also exert influence on proton **6**′. In fact, ring currents effects have been commonly observed in several bis(bipyridyl)ruthenium complexes.[30] In our case, an interesting feature is the signal located at 10.08 ppm, ascribed to proton **10**′. In the $[Ru(bpy)_2Cl(BPEB)]^+$ complex, this proton is located just above the Cl^- ion and is shifted downfield by almost 2 ppm in relation to the same proton in $[Ru(bpy)_3]^{+2}$. Large downfield shifts have been observed in many bis(bipyridine)ruthenium chloride complexes arising from the inductive effect of the Cl^- ion on the adjacent proton.[33,34]

The differenciation of the two pyridyl ring protons, such as **9** and **9**′, was carried out on the basis of the ^{1}H$-^1$H COSY spectrum (not shown). Proton **10**′ was employed in the assignment of the **7**′, **8**′, **9**′, and **10**′ ring, while, similarly, proton **10** was employed to assign the **7**, **8**, **9**, and **10** ring. At this point, the ^{1}H$-^1$H COSY spectrum has allowed us to assign only a single bipyridyl ligand. The assignment of the other bipyridyl and BPEB ligands was carried out by means of correlation with the ^{13}C NMR and ^{1}H$-^{13}$C HMQC spectra. The ^{13}C chemical shifts for both complexes were assigned by comparison with analogous compounds,[30−32] and the total assignment of ^{1}H NMR spectra was carried out using the ^{1}H$-^{13}$C HMQC correlation spectrum (data available as Supporting Information).

Table 1. Electrochemical Data for the $[Ru(bpy)_2Cl(BPEB)]^+$ and $\{[Ru(bpy)_2Cl]_2(BPEB)\}^{2+}$ Complexes in DMF and 0.1 mol dm^{-3} $(TBA)PF_6$

	$E_{1/2}$ (V vs SHE)		
compd	$BPEB^{2-/-}$ ($bpy^{-/0}$)	$BPEB^{-/0}$ ($bpy^{-/0}$)	$Ru^{2+/3+}$
$[Ru(bpy)_2Cl(BPEB)]^+$	−1.15	−1.02	1.18
$\{[Ru(bpy)_2Cl]_2(BPEB)\}^{2+}$	−1.15 (−1.15)	−0.97 (−0.97)	1.20
BPEB	−1.61	−1.48	

Electrochemical Measurements. Cyclic and differential pulse voltammograms of free BPEB ligand consist of two successive, reversible, monoelectronic processes centered at −1.48 and −1.61 V, which can be ascribed to $BPEB^{\bullet-/0}$ and $BPEB^{2-/\bullet-}$, respectively. The spectroelectrochemical behavior associated with these two processes is shown in Figure 3. The first reduction of the BPEB ligand leads to the decay of the $\pi \rightarrow \pi^*$ band at 356 nm and to the rise of strong absorption bands at 646 and 1100 nm, ascribed to $\pi \rightarrow \pi^*$ transitions in the corresponding radical anion species (Figure 3a). Similar responses were observed for the radical anions of 2,2′-bipyridine and/or 2,2′-bipyrimidine radical anion species.[35] In fact, preliminary theoretical calculations for the BPEB ligand using the PM3 method has shown that the added, unpaired electron is delocalized all over the ligand. The next, successive one-electron reduction generating the BPEB bianion leads to the decay of the absorption bands at 646 and 1100 nm (Figure 3b).

The voltammogram profiles for the mononuclear and binuclear complexes exhibit three sets of waves as shown in Figure 4. The corresponding $E_{1/2}$ values were collected in Table 1. In comparison with analogous poly(pyridyl)ruthenium complexes,[36] the ruthenium-centered redox processes are significantly shifted to more positive values (ΔE > 160 mV), reflecting the π-acceptor nature of the BPEB ligand. Interestingly, there is no evidence of splitting in the $Ru^{3+/2+}$ redox waves of the binuclear complex, indicating that, despite the highly conjugated properties of the BPEB ligand, the electronic coupling between the two metal centers remains quite small. The DPV voltammograms profiles for both complexes exhibited significant differences in the current peak intensities. For the mononuclear complex the DPV pattern is consistent with involvement of the same number of electrons in the three redox processes, while for

(31) Maruyama, M.; Matsuzawa, H.; Kaizu, Y. *Inorg. Chim. Acta* **1995**, *237*, 159.
(32) Constable, E. C.; Seddon, K. R. *Inorg. Chim. Acta* **1983**, *70*, 251.
(33) Leising, R. A.; Kubow, S. A.; Churchill, M. R.; Buttrey, L. A.; Ziller, J. W.; Takeuchi, K. J. *Inorg. Chem.* **1990**, *29*, 1306.
(34) Heijden, M.; van Vliet, P. M.; Haasnoot, J. G.; Reedijk, J. *J. Chem. Soc., Dalton Trans.* **1993**, 3675.
(35) Bates, W. D.; Chen, P.; Bignozzi, C. A.; Schoonover, J. R.; Meyer, T. J. *Inorg. Chem.* **1995**, *34*, 6215.
(36) Powers, M. J.; Meyer, T. J. *J. Am. Chem. Soc.* **1980**, *13*, 1289.

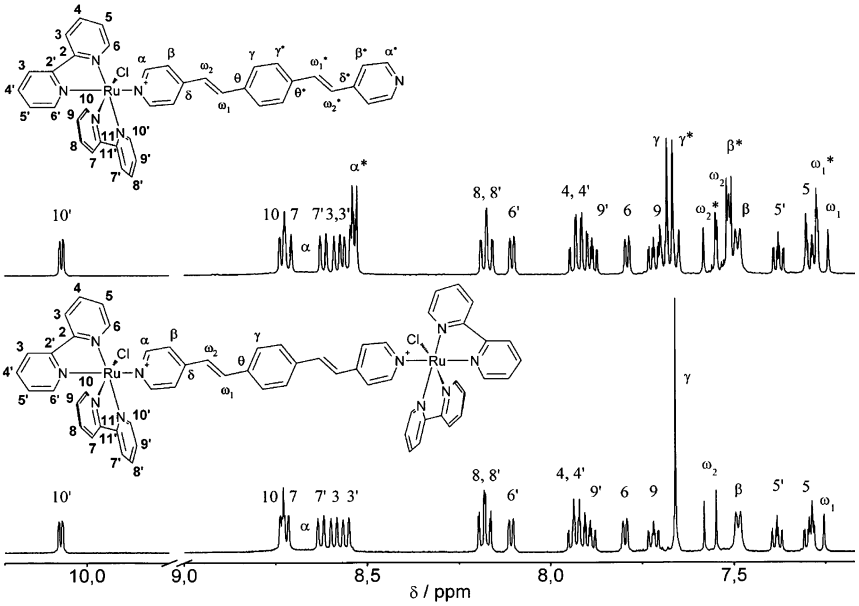

Figure 2. ^{1}H NMR spectrum of mono- and binuclear ruthenium complexes (10^{-2} mol dm^{-3}) in $(CD_3)_2CO$.

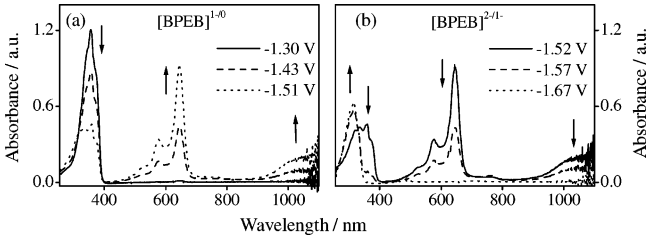

Figure 3. Spectroelectrochemical behavior of the BPEB bridging ligand in DMF solution. The potential ranges are indicated.

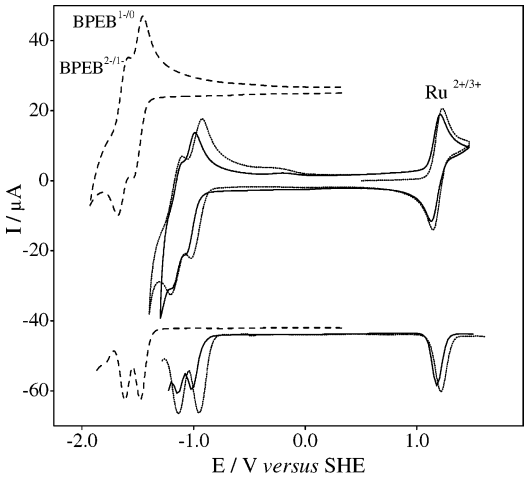

Figure 4. Cyclic and differential pulse voltammograms of the BPEB free ligand (dashed line), $[Ru(bpy)_2Cl(BPEB)]^+$ (solid line), and $\{[Ru(bpy)_2Cl]_2(BPEB)\}^{2+}$ complexes (dotted line) in DMF and 0.1 mol dm^{-3} $(TBA)PF_6$ at room temperature.

the binuclear complex the peaks at −1.15, −1.07, and 1.20 V exhibited 3:3:2 intensity ratios, suggesting a possible overlap of the BPEB and bipy reduction processes below −1.0 V.

Spectroelectrochemical measurements for the $[Ru(bpy)_2Cl(BPEB)]^+$ and $[\{Ru(bpy)_2Cl\}_2(BPEB)]^{2+}$ complexes are shown in Figure 5. The starting complexes exhibited characteristic absorption bands at 297 and 355 nm, ascribed to $\pi \rightarrow \pi^*$ transitions in the bpy and BPEB, ligands,

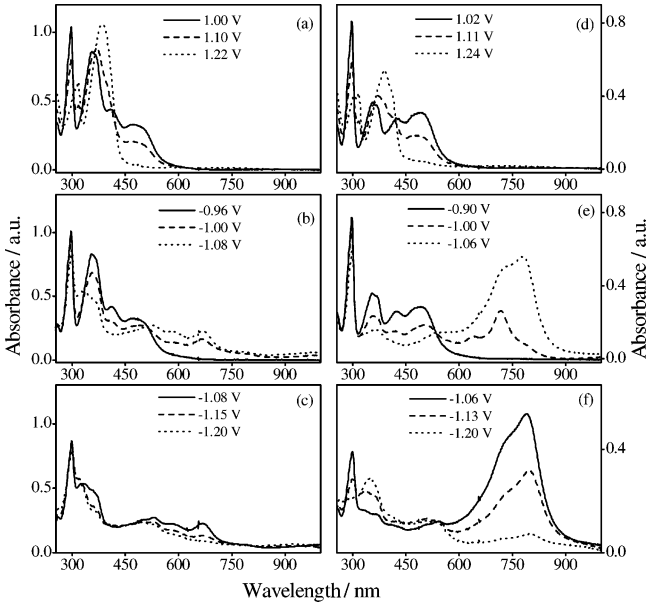

Figure 5. Spectroelectrochemical behavior of $[Ru(bpy)_2Cl(BPEB)]^+$ (a−c) and $\{[Ru(bpy)_2Cl]_2(BPEB)\}^{2+}$ (d−f), in DMF solution. The potential ranges are indicated.

respectively. In addition, metal-to-ligand charge transfer (MLCT) bands were located at 412 and 471 nm in the mononuclear and at 426 and 489 nm in the dinuclear species, respectively.

As shown in Figure 5a, in the 1.00−1.22 V range, the $Ru^{2+/3+}$ redox process leads to the decay of the metal-to-ligand charge transfer (MLCT) bands of the mononuclear complex, whereas the BPEB band undergoes a bathochromic shift from 356 to 386 nm. The binuclear complex exhibits a similar behavior, as shown in Figure 5d.

A contrasting result was observed in the reduction processes for the two complexes, as indicated in Figure 5b,c and Figure 5e,f, respectively. For the mononuclear complex, the first reduction process at −1 V led to the decay of the BPEB $\pi \rightarrow \pi^*$ band at 356 nm (Figure 5b) and to the rise

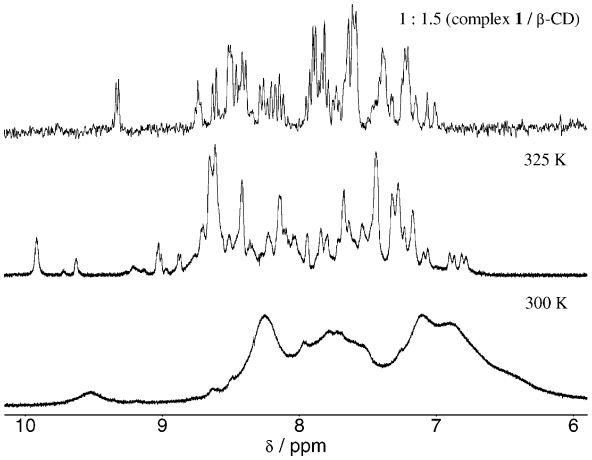

Figure 6. Temperature dependence ^{1}H NMR data for the $[Ru(bpy)_2Cl(BPEB)]^+$ complex (10^{-2} mol dm^{-3}) in D_2O solution and ^{1}H NMR titration of the complex **1** with β-CD at 298 K (top).

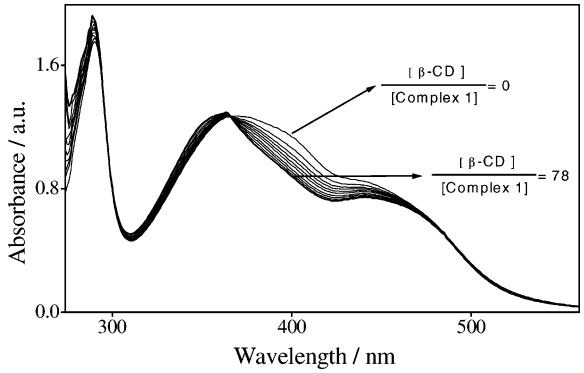

Figure 7. UV−visible spectra showing the effect of addition of β-CD to the mononuclear complex in aqueous media containing 0.1 M NaCl, 25 °C. The concentration of mononuclear complex was kept constant at 3.12 × 10^{-5} mol dm^{-3}, and that of β-CD varied from 0.28 × 10^{-3} to 2.42 × 10^{-3} mol dm^{-3}.

of new bands around 660 and 1000 nm, consistent with BPEB radical anion spectrum. The following step at −1.15 V (Figure 5c) led to the decay of such bands, as observed for the second one-electron reduction of the BPEB ligand. In the case of the binuclear complex, as shown in Figure 5e, the reduction process at −1 V led initially to the decay of the BPEP $\pi \rightarrow \pi^*$ band at 355 nm, with the rise of the characteristic BPEB radical anion band at 718 nm. This process was followed by the decay of the bpy $\pi \rightarrow \pi^*$ band at 297 nm leading to a new band at 781 nm, evidencing the reduction of the bpy ligand. Finally, in the −1.08 to −1.20 V range, there is a simultaneous decay of the absorption bands at 297, 718, and 781 nm, indicating the reduction to $BPEB^-$ and bpy^- ligands, respectively. The simultaneous reduction of the BPEB and bipy ligands in the binuclear complex corroborates the results from the DPV experiments shown in Figure 4.

^{1}H NMR Studies Focusing on Aggregation and Inclusion into β-Cyclodextrin. Aggregation of complexes promoted by π-stacking of the polyaromatic ligands has already been reported in the literature.[21,37,38] In this work we have observed that, in D_2O solutions, all the ^{1}H NMR peaks (corresponding to BPEB and bpy ligands) for the mononuclear complex are broadened and unresolved, contrasting with the corresponding ^{1}H NMR spectra in $(CD_3)_2CO$ solution, reflecting an aggregation phenomena.

In Figure 6, it is shown the ^{1}H NMR spectra of the mononuclear complex at two different temperatures and in the presence of β-CD. At 300 K, in the range of concentration from 1 to 10 mmol dm^{-3}, in D_2O, the aromatic protons give rise to very broad peaks. By the increasing of temperature to 325 K, these peaks become sharp and resolved (Figure 6b), showing the collapse of the aggregated structure.

It is interesting to note that the both BPEB and bpy signals undergo downfield shifts as the temperature is increased up to 325 K. This result reflects the collapse of the $[Ru(bpy)_2Cl(BPEB)]^+$ aggregate, where the downfield shifts result from the rupture of the π aromatic apolar environment (deshielding) accompanying the dissociation of the $\pi-\pi$ stackings. More interesting is the fact that the addition of β-CD to a solution containing the mononuclear complex, in the aggregated form, resulted in sharp ^{1}H NMR peaks, as one can see in Figure 6b. Such changes evidenced the inclusion of the hydrophobic BPEB residue of the $[Ru(bpy)_2Cl(BPEB)]^+$ complex into the β-CD cavity. An inclusion complex between the free ligand BPEB and β-CD has also been observed in D_2O solutions, exhibiting 1:1 binding stoichiometry.

To characterize the inclusion process, the corresponding stoichiometry was determined by means of the continuous variation method (Job plot),[25] as described in the Experimental Section. By the plotting of $\Delta\delta$ [β-CD] against r (molar fraction of the host), the maximum occurred at r = 0.5, indicating 1:1 stoichiometry for the inclusion complex $[Ru(bpy)_2Cl(BPEB\cdot\beta\text{-CD})]^+$.

Determination of the Association Constant. In water, at concentrations below 4 × 10^{-5} mol dm^{-3}, the mononuclear complex exhibited no significant changes in the absorption profiles, ruling out the contribution of the aggregation phenomena, at this dilution level. However, the addition of β-CD (L) leads to hypsochromic shift of the BPEB ligand $\pi \rightarrow \pi^*$ transition from 370 to 363 nm (Figure 7) indicative of the formation of the inclusion complex $[Ru(bpy)_2Cl(BPEB\cdot\beta\text{-CD})]^+$ (SL).

The spectral changes in Figure 7 show well-defined isosbestics points that are preserved over the full range of β-CD concentrations, indicating that only a single stoichiometry is involved. The association constant for the mononuclear complex was calculated from the linear plots $\Delta A/[S]$ against $-\Delta A$ (the absorbance changes at 440 nm). $\Delta\epsilon_{SL}$ was obtained by extrapolation to infinite diluted solution as 1.15 ± 0.1 × 10^4 cm^{-1} mol^{-1} dm^3, and from the slope, K_a was calculated as 872 ± 8 M^{-1}. This is comparable to those (e.g. varying from 150 to 1040 M^{-1}) observed for inclusion compounds of 4,4′-bipy and related complexes and β-CD.[13,16−19]

Conformational Analysis by NMR Spectroscopy. Additional information on the $[Ru(bpy)_2Cl(BPEB.\beta\text{-CD})]^+$

(37) Gourdon, A.; Launay, J.-P. *Inorg. Chem.* **1998**, *37*, 5336.
(38) Franco, M.; Araki, K.; Rocha, R. C.; Toma, H. E. *J. Solution Chem.* **2000**, *29*, 667.

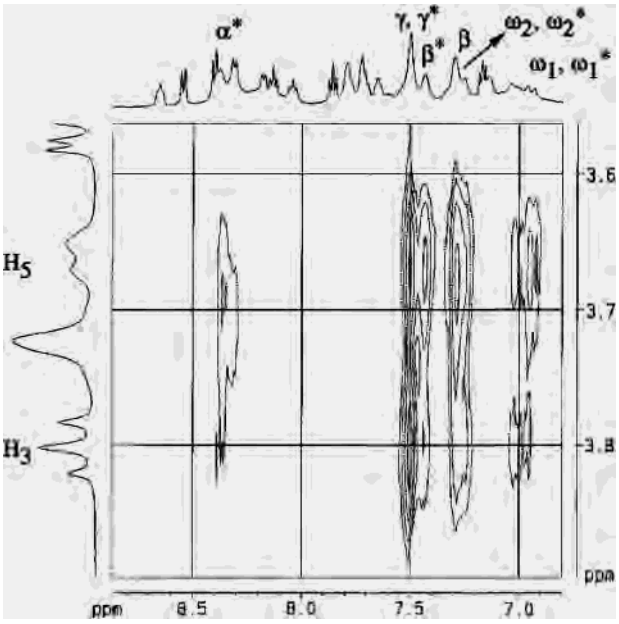

Figure 8. Partial NOESY correlation map of the inclusion complex with β-CD at 27 °C in D_2O.

inclusion complex has been obtained from the ^{1}H NMR chemical shifts in D_2O. In the β-CD ^{1}H NMR the internal H_3 and H_5 signals are strongly sensitive to the electronic environment inside the cavity. These changes are modulated by the features of the aromatic guest included by the host. In the $[Ru(bpy)_2Cl(BPEB)]^+$ case, the inclusion results on upfield shifts of the internal H_3 and H_5 protons of the β-CD molecule, induced by the ring currents from the aromatic BPEB residues inside the cavity.

To obtain more detailed information, the inclusion complex was investigated by means of two-dimensional nuclear Overhauser enhancement (NOESY). The nuclear Overhauser enhancement (NOE) is a manifestation of cross-relaxation between two nonequivalent nuclear spins which are close enough, e.g. <5 Å (through space). The partial NOESY correlation map of the inclusion complex with β-CD is shown in Figure 8.

For the $[Ru(bpy)_2Cl(BPEB\cdot\beta\text{-CD})]^+$ complex, strong intermolecular cross-magnetizations between the H_3 and H_5 protons located inside the β-CD cavity and the α, α*, β, β*, γ, γ*, ω_1, ω_1*, and ω_2, ω_2* BPEB protons were observed. This observation suggest that the binuclear complex is included into the β-CD cavity through the BPEB portion, since only NOE correlation between their nuclei has been observed. In addition, the NOESY spectrum reveals that the remote portion of the BPEB ligand (β*, γ, γ*, ω_1*, and ω_2* protons) binds more tightly.

Conclusions

The linear, conjugated *trans*-1,4-bis[2-(4-pyridyl)ethenyl]-benzene) ligand forms an interesting mononuclear complex with ruthenium(II) polypyridine species, exhibiting strong $\pi-\pi$ stacking interactions responsible for extensive aggregation in aqueous solution. In the presence of β-CD a stable inclusion complex is obtained, breaking down the aggregation tendency in aqueous solution. This type of intermolecular interaction has not been detected in the binuclear complex. The electrochemical behavior of this species differs from that for the mononuclear ones, from the occurrence of redox processes involving the bipyridine ligands overlapping those characteristic of the BPEB ligand. Because of the intermolecular interactions, the mononuclear species provide interesting applications in supramolecular chemistry, allowing molecular recognition by forming inclusion compounds, as well as self-assembling processes in the presence of suitable partners exhibiting a π-stacking response.

Acknowledgment. We gratefully acknowledge the financial support from the Brazilian agencies CNPq and FAPESP and the Institute of Millennium for Complex Materials.

Supporting Information Available: ^{1}H and ^{13}C NMR data for the mononuclear and binuclear complexes. This material is available free of charge via the Internet at http://pubs.acs.org.

IC0352250